P–δ Characteristics for the Unified Power Flow Controller—Analysis Inclusive of Equipment Ratings and Line Limits

J. Z. Bebic, *Member, IEEE*, P. W. Lehn, *Member, IEEE*, and M. R. Iravani, *Senior Member, IEEE*

***Abstract*—The paper presents a direct and systematic method for determining the entire operating range of a UPFC in the presence of equipment and system operating limits. The method is inclusive of all limits: series converter voltage and current limits, shunt converter current limit, and voltage limits at the equipment terminals. The formulation is general and permits calculation of P–δ curves for a UPFC installed at any point along the transmission line. Equipment and system operating limits are shown to significantly impact the P–δ curves of the UPFC. The methodology presented in the paper provides system planners a means to realistically quantify potential benefits of a UPFC installation for a transmission system.**

***Index Terms*—FACTS, P–delta curves, power system dynamic stability, UPFC.**

I. Introduction

THE UNIFIED power flow controller (UPFC) enables independent and simultaneous control of a transmission line voltage, impedance, and phase angle [1]. This has far reaching benefits: in steady state, the UPFC can be used to regulate the power flow through the line and improve utilization of the existing transmission system capacity; and, during power system transients, the UPFC can be used to mitigate power system oscillations and aid in the first swing stability of interconnected power systems [2].

Currently, time domain simulation techniques which require exhaustive number of trial runs are the only tool available for analysis of a general UPFC in the presence of practical equipment and system limits.

For effective system planning, a UPFC model requires the following features: The model must be sufficiently general to permit evaluation of UPFC placement anywhere within a transmission line, not only at sending or receiving ends. Furthermore, the model should allow the UPFC to have any orientation within the line (i.e., with the series converter on either the sending or receiving side of the shunt converter). Standard operational limits on the system and the UPFC converters need also be considered. Primarily, these include limits on the series converter voltage and current, the shunt converter current limit, and voltage limits at the equipment terminals. To date, no analytic model is available which offers all of these features.

Manuscript received September 23, 2002.

The authors are with the Department of Electrical and Computer Engineering, University of Toronto, ON M5S 3G4, Canada (e-mail: jovan.bebic@utoronto.ca; lehn@ecf.utoronto.ca; iravani@ecf.utoronto.ca).

Digital Object Identifier 10.1109/TPWRD.2003.813610

Over the years, researchers have, however, made progress on less general UPFC modeling aspects. In [3], the authors have modeled the shunt converter of a UPFC as a parallel connection of a controllable shunt admittance and a current source that draws only active power. P–δ curves were plotted, but the voltage limits at the equipment terminals, and current ratings of the converters were not considered. Notably, this is one of the few papers that examines the possibility of installing a UPFC within the line (i.e., at a point where the UPFC is connected to relatively long transmission line segments at both its input and output terminals).

In [4], a model of the UPFC based on two voltage-sourced converters was developed. A reachable set of operating points was examined in the P–Q plane using combined iterations of a load flow program and numerical methods to solve for the operating parameters of the UPFC. A limitation of this approach is that current ratings of the converters are not considered.

In [5], a model of the UPFC based on a shunt connected current source and series voltage source was developed. An assumed point of installation at the beginning of the transmission line enabled application of all limits throughout the analysis.

A major limitation of the proposed method is that it assumes the connection of the shunt converter to a stiff voltage source; therefore, the technique is not directly applicable to a UPFC with a point of installation within the line.

This paper describes a direct and systematic method for determining the entire reachable set of operating points for a line controlled by a UPFC. The analysis is valid for any point of UPFC installation in the line, and permits application of all relevant limits (i.e., series converter voltage and current magnitudes are limited, shunt converter current is limited, voltage limits at equipment terminals are respected). The analysis method is graphical, and therefore, provides direct insight into how various limits constrain the operating region of the UPFC. Moreover, it provides a straightforward approach to find the operating point that maximizes (minimizes) the power flow. The procedure is used to deduce the P–δ curves of a UPFC and to demonstrate how various limit conditions constrain its operating region.

II. General Statement of the Problem

A schematic diagram of the studied system is shown in Fig. 1. The UPFC is installed at an arbitrary point within the transmission line. Equivalent reactances between the sending end voltage ($\mathbf{V_S}$) and the input terminal of the UPFC ($\mathbf{V_{ET}}$), and

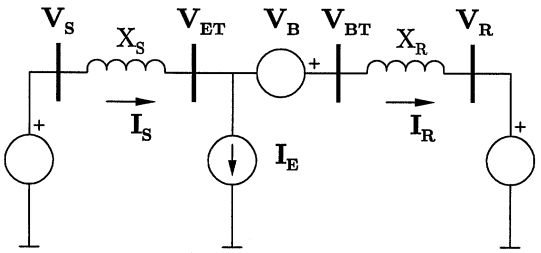

Fig. 1. Simplified representation of the line controlled by the UPFC.

between the output terminal of the UPFC ($\mathbf{V_{BT}}$) and the receiving end voltage ($\mathbf{V_R}$) are denoted X_S and X_R, respectively. X_S and X_R include transformer leakage reactances and machine reactances of the system. In addition, X_R also includes the leakage reactance of the UPFC series transformer. In general, $X_S \neq X_R$. The UPFC is represented by a shunt current source ($\mathbf{I_E}$), and the series voltage source ($\mathbf{V_B}$). As the model suggests, all losses (line and converters) will be neglected to help maintain the emphasis of the discussion on the analysis.

The objective of the analysis is to find all operating points of the system while respecting limits imposed by the ratings of the installed converters, and voltage limits at the equipment terminals. The following limits will be considered:

$$|\mathbf{V_B}| \leq \mathrm{V_{B\,max}} \tag{1}$$

$$|\mathbf{I_R}| \leq \mathrm{I_{B\,max}} \tag{2}$$

$$|\mathbf{I_E}| \leq \mathrm{I_{E\,max}} \tag{3}$$

$$|\mathbf{V_{ET}}| \leq \mathrm{V_{ET\,max}} \tag{4}$$

$$|\mathbf{V_{BT}}| \leq \mathrm{V_{BT\,max}}. \tag{5}$$

Inequalities (1) and (2) represent the voltage and current limit of the series converter. Inequality (3) represents the current limit of the shunt converter. Finally, (4) and (5) represent the voltage limits on the equipment terminals. Should it be required, lower limits on one or both terminal voltages can also be applied [limit condition (4) would then take the form $V_{\min} \leq |\mathbf{V_{ET}}| \leq V_{\max}$].

Imposing limits on both the shunt current and the UPFC terminal voltage, $\mathbf{V_{ET}}$ directly limits the required shunt converter voltage.

The UPFC consists of two converters that share a common dc circuit. If there is no energy storage device coupled to the dc circuit, then, in steady state operation, the active power exchanged between the series converter and the line must be supplied (discharged) by the shunt converter. Equation (6) describes this condition

$$\mathrm{Re}\,(\mathbf{V_{ET}} \cdot \mathbf{I_E^*}) = \mathrm{Re}\,(\mathbf{V_B} \cdot \mathbf{I_R^*}). \tag{6}$$

This condition introduces nonlinearity to the mathematical model of the UPFC, and adds significant complexity to the problem.

III. Graphical Interpretation of Power Balance

A graphical method for solving the nonlinear power balance equation is presented in this section. It leads to the definition of a new coordinate system that facilitates calculation of the UPFC operating region.

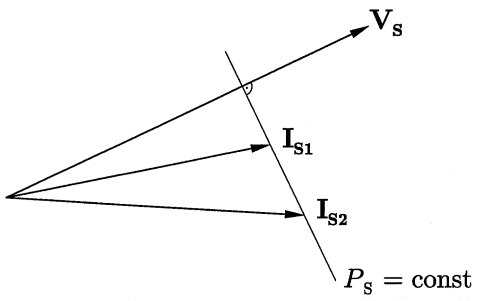

Fig. 2. Constant power line.

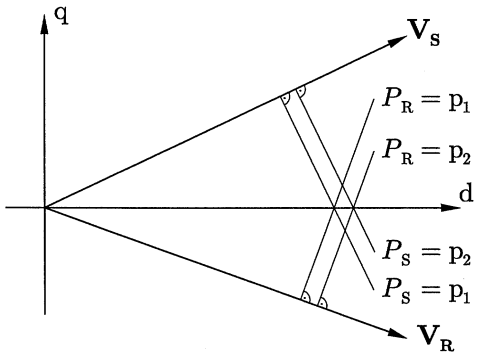

Fig. 3. Lines of equal sending and receiving end power.

The condition of power balance between the shunt and series converter implies that a UPFC, considered as a "black box," does not exchange active power with the rest of the system. In steady state, the active power supplied at the sending end of the line is all absorbed by the receiving end.

Consider first the sending end power. The active power is proportional to the projection of the sending end current vector onto the sending end voltage vector, as shown in Fig. 2. Therefore, current vectors $\mathbf{I_{S1}}$ and $\mathbf{I_{S2}}$ transfer the same sending end power, as would any other current vector that has its tip on the same line perpendicular to $\mathbf{V_S}$. This line will be called a "constant power line."

Fig. 3 shows two constant power lines for the sending end. It also shows the two constant power lines for the receiving end that correspond to the same power flows. Thus, if $\mathbf{I_S}$ lies anywhere on the $P_S = p_1$ line, then power balance requires $\mathbf{I_R}$ to lie somewhere on the $P_R = p_1$ line. When multiple pairs of constant power lines are drawn, the locus of their intersection points defines a line. Let this line define the d-axis of the proposed d–q coordinate system of Fig. 3.

The motivation for choosing this coordinate system is that it provides a straightforward geometrical interpretation of the power transfer through the line. Changing the power transfer through the line corresponds to horizontally translating a pair of equal power lines along the d-axis. That is, the power transfer is proportional to the d coordinate of the point of intersection of equal power lines. Thus, in Fig. 3, $p_2 > p_1$. Notice that the orientation of the d-axis also corresponds to the orientation of the line current before any compensation.

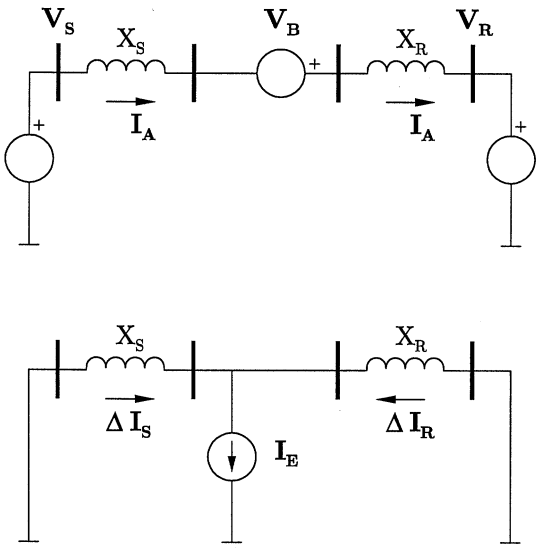

Fig. 4. Decomposition of the original circuit.

IV. Circuit Decomposition

The circuit of Fig. 1 can be decomposed, based on the principle of superposition, into two circuits shown in Fig. 4. This permits independent analysis of influence of series and shunt converter on $\mathbf{I_S}$ and $\mathbf{I_R}$. Comparing Figs. 1 and 4 it can be deduced

$$\mathbf{I_S} = \mathbf{I_A} + \mathbf{\Delta I_S} \tag{7}$$

$$\mathbf{I_R} = \mathbf{I_A} - \mathbf{\Delta I_R}. \tag{8}$$

Let X_S and X_R be expressed using the total circuit reactance X_L and a factor k

$$X_S = kX_L \tag{9}$$

$$X_R = (1-k)X_L. \tag{10}$$

Factor k quantifies the "electrical distance" between the sending end of the line and the UPFC. Expressions for current components of (7) and (8) are

$$\mathbf{I_A} = \frac{\mathbf{V_S} - \mathbf{V_R}}{jX_L} + \frac{\mathbf{V_B}}{jX_L} \tag{11}$$

$$\mathbf{\Delta I_S} = (1-k)\mathbf{I_E} \tag{12}$$

$$\mathbf{\Delta I_R} = k\mathbf{I_E}. \tag{13}$$

$\mathbf{I_A}$ is composed of $\mathbf{I_0}$ and $\mathbf{I_B}$, defined as

$$\mathbf{I_0} = \frac{\mathbf{V_S} - \mathbf{V_R}}{jX_L} \tag{14}$$

$$\mathbf{I_B} = \frac{\mathbf{V_B}}{jX_L}. \tag{15}$$

The composition of $\mathbf{I_A}$ is shown in Fig. 5. $\mathbf{I_A}$ resides within the circle centered at $\mathbf{I_0}$ and with a radius specified by the voltage limit of the series converter, as per (15). This circle will be called the "$\mathbf{I_A}$ circle." $\mathbf{I_A}$ circle gives a graphical interpretation to inequality (1).

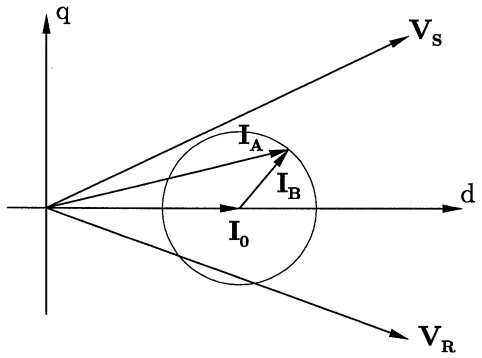

Fig. 5. Reachable set of line current before shunt injection.

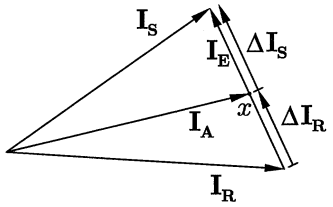

Fig. 6. Vectorial composition of $\mathbf{I_S}$ and $\mathbf{I_R}$.

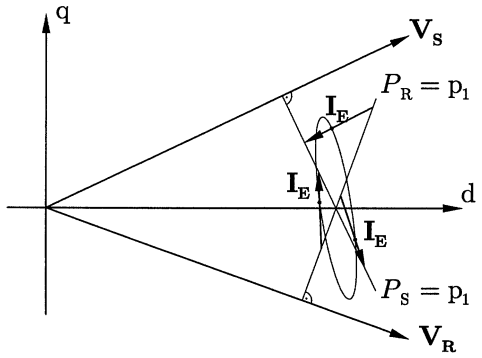

Fig. 7. Family of solutions for $\mathbf{I_E}$ and $\mathbf{I_A}$.

According to (12) and (13), $\mathbf{\Delta I_S}$ and $\mathbf{\Delta I_R}$ are co-linear, and their sum is equal to $\mathbf{I_E}$. However, $\mathbf{I_E}$ is also the difference between $\mathbf{I_S}$ and $\mathbf{I_R}$, as shown in Fig. 6. Hence, the solution pair ($\mathbf{I_S}$, $\mathbf{I_R}$) can be viewed as a special composition of $\mathbf{I_A}$ and $\mathbf{I_E}$, where the tip of $\mathbf{I_A}$ lies on $\mathbf{I_E}$. This "point of contact" is denoted as "x" in Fig. 6. Location of point "x" on $\mathbf{I_E}$ is uniquely determined by the factor k.

The relation of Fig. 6 therefore imposes an additional constraint on $\mathbf{I_A}$. As determined in the previous section, power balance stipulates that $\mathbf{I_S}$ and $\mathbf{I_R}$ lie on a pair of constant power lines. Thus, for a given power transfer, p_1 the tip of $\mathbf{I_E}$ must lie on the constant power line $P_S = p_1$, and its tail on the line $P_R = p_1$. For a given amplitude of $\mathbf{I_E}$, a family of possible solutions for $\mathbf{I_E}$ exists, as shown in Fig. 7. The tip of each associated $\mathbf{I_A}$ vector must lie at point "x" on the $\mathbf{I_E}$ vector. These points are marked by dots on $\mathbf{I_E}$ vectors. The locus of all possible $\mathbf{I_A}$ vectors (corresponding to the given power transfer p_1, and a given amplitude of the vector $\mathbf{I_E}$) is an ellipse as shown in Fig. 7.

Power balance therefore requires the tip of $\mathbf{I_A}$ to lie on an ellipse. Notice that power transfer p_1 determines the d coordinate of the ellipse's center, but it does not change its shape and orientation. The ellipse that corresponds to $p_1 = 0$ can be described by the parametric equation

$$\begin{bmatrix} x_d \\ x_q \end{bmatrix} = \mathbf{R}(\theta) \cdot |\mathbf{I_E}| \cdot \begin{bmatrix} a & 0 \\ 0 & b \end{bmatrix} \cdot \begin{bmatrix} \cos(\xi) \\ \sin(\xi) \end{bmatrix} \tag{16}$$

where "ξ" is the parameter taking values in the set: $[0, 2\pi]$ and $\mathbf{R}(\theta)$ is the rotation matrix defined as

$$\mathbf{R}(\theta) = \begin{bmatrix} \cos(\theta) & -\sin(\theta) \\ \sin(\theta) & \cos\theta \end{bmatrix}. \tag{17}$$

The angle θ is defined as

$$\theta = \delta_R + \alpha - \pi/2 \tag{18}$$

where δ_R is the angle between $\mathbf{V_R}$ and the d-axis, and α is given by (19)

$$\tan(2\alpha) = \frac{k\sin(2\delta)}{1 - 2k\sin(\delta)^2}. \tag{19}$$

The quadrant of the solution is determined from

$$\text{sign}\,(\sin(2\alpha)) = \text{sign}\,(\cos(\delta)). \tag{20}$$

Lengths of major and minor axis are given as

$$a = c + d \tag{21}$$

$$b = c - d. \tag{22}$$

Constants c and d are

$$c = \frac{1}{2\sin(\delta)} \tag{23}$$

$$d = \frac{1}{2}\sqrt{\frac{1}{\sin(\delta)^2} - 4k(1-k)} \tag{24}$$

where δ is the angle between $\mathbf{V_S}$ and $\mathbf{V_R}$.

An operating region can exist, if and only if the circle constraint on $\mathbf{I_A}$ as well as the ellipse constraint on $\mathbf{I_A}$ have a common area.

Note the following important results: (1) is satisfied by choosing the appropriate radius of the $\mathbf{I_A}$ circle; (3) is satisfied by limiting the value of $|\mathbf{I_E}|$ used in the ellipse equation; and the condition of power balance is satisfied inherently through definition of the ellipse, that is, by forcing the ends of the vector $\mathbf{I_E}$ to reside on equal power lines.

To summarize, the method presented provides a powerful tool to seek the solutions for $\mathbf{I_S}$ and $\mathbf{I_R}$ that reside on a manifold defined by the condition of equal power exchange between the converters. Hence, the nonlinearity due to (6) is eliminated, making a general analysis possible. In the next section, this methodology will be used to solve for the operating points associated with the minimum and maximum power flow. A method to impose limit conditions (2), (4), and (5) will also be presented.

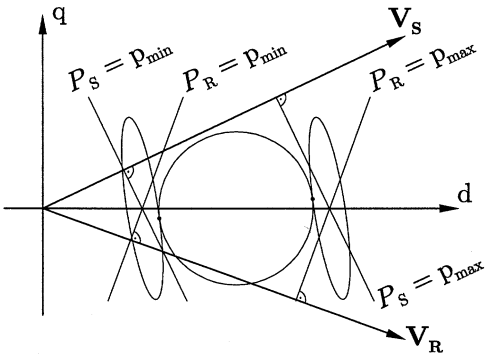

Fig. 8. Geometric interpretation of the minimum and maximum power flow.

V. Minimum and Maximum Power Flow

Section III explained that changing the transmitted power through the line corresponds to translating the point of intersection of equal power lines along the d-axis. This results in translation of the ellipse circumscribed by point "x" on $\mathbf{I_E}$. Any valid solution pair ($\mathbf{I_S}$, $\mathbf{I_R}$) requires the tip of $\mathbf{I_A}$ to coincide with point "x" on $\mathbf{I_E}$. Maximum power flow is therefore obtained when the ellipse is translated in positive direction until it is tangent to the $\mathbf{I_A}$ circle. Conversely, the minimum power flow is realized when the ellipse is translated in negative direction until it is tangent to the $\mathbf{I_A}$ circle from the other side. These two conditions are graphically shown in Fig. 8.

VI. Additional Limits

It was stated that solution pairs obtained using the proposed process only meet power balance and limit conditions (1) and (3). Nonetheless, remaining limit conditions can be imposed as follows.

Currents $\mathbf{I_S}$ and $\mathbf{I_R}$ can be expressed as

$$\mathbf{I_S} = \frac{\mathbf{V_S}}{jkX_L} - \frac{\mathbf{V_{ET}}}{jkX_L} \tag{25}$$

$$\mathbf{I_R} = -\frac{\mathbf{V_R}}{j(1-k)X_L} + \frac{\mathbf{V_{BT}}}{j(1-k)X_L}. \tag{26}$$

Examination of these expressions reveals that the limits specified by (4) and (5) can be represented as circles in the current space, as depicted in Fig. 9. The first terms in (25) and (26) define the location of the circle centers, while the limit conditions (4) and (5) define their radii. $\mathbf{I_S}$ is therefore constrained to lie within the $V_{ET\max}$ circle marked in Fig. 9, while $\mathbf{I_R}$ is constrained to lie within the $V_{BT\max}$ circle. Finally, the series converter current limit is represented by a circle centered at the origin with radius $I_{B\max}$. For the UPFC orientation shown in Fig. 1, it is the receiving end current $\mathbf{I_R}$ that must lie within the $I_{B\max}$ circle. These additional constraints may indirectly limit the magnitude of $\mathbf{V_B}$ to some value less than $V_{B\max}$, and the magnitude of $\mathbf{I_E}$ to some value less than $I_{E\max}$.

Application of these limits will be illustrated through the following example: Suppose that $\mathbf{V_S}$, $\mathbf{V_R}$, circuit parameters, equipment limits, and line limits are given. Take a specific value

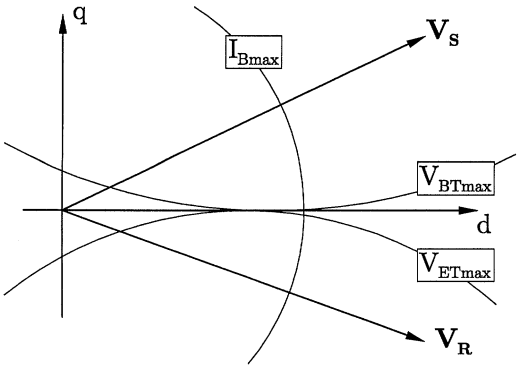

Fig. 9. Illustration of additional limit boundaries.

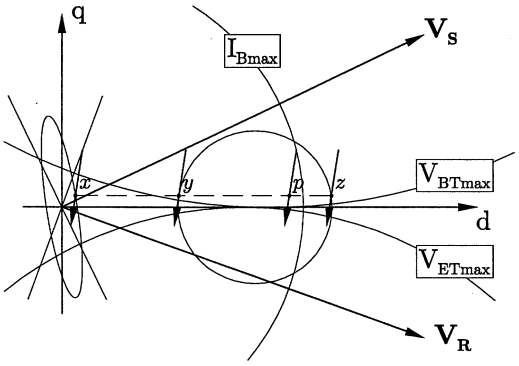

Fig. 10. Example illustrating application of the additional limits.

of $\mathbf{I_E}$ such that $|\mathbf{I_E}| \in [0,\ I_{E\max}]$. Solve for all possible steady state operating points of the UPFC under these conditions.

The solution for this problem is explained based on Fig. 10. Fig. 10 is an extension of Fig. 9; therefore, only the additional elements will be discussed. In Fig. 10, an ellipse that corresponds to zero power transfer and a given amplitude $|\mathbf{I_E}|$ is shown centered at the origin of the d–q coordinate system. Along with it are shown the equal power lines, and the specific $\mathbf{I_E}$ that is being considered. The $\mathbf{I_A}$ circle is also shown.

Changing the transmitted power results in translation of the ellipse. Specifically, this results in the translation of $\mathbf{I_E}$, and its associated point "x". Corresponding trajectory of "x" is a straight line—shown dashed in Fig. 10. This line intersects with the $\mathbf{I_A}$ circle at points "y" and "z." Power balance stipulates that the tip of $\mathbf{I_A}$ contacts $\mathbf{I_E}$ at "x"; hence, the tip of $\mathbf{I_A}$ lies on line segment $\overline{yz}$. Limit conditions discussed in this section require that $\mathbf{I_S}$ and $\mathbf{I_R}$ lie within their respective limit circles. Based on Fig. 6, the tip of $\mathbf{I_S}$ coincides with the tip of $\mathbf{I_E}$, while the tip of $\mathbf{I_R}$ coincides with the tail of $\mathbf{I_E}$. Therefore, the tip of $\mathbf{I_E}$ must lie within the circle labeled: $V_{ET\max}$, and its tail within the circles labeled: $V_{BT\max}$ and $I_{B\max}$. In Fig. 10, "p" is the point on $\overline{yz}$ farthest to the right that still respects the current limit. Hence, it yields the solution associated with the maximum power flow for the given point "x." Point "y" is associated with the minimum power flow.

This example illustrates that application of $V_{ET\max}$, $V_{BT\max}$, and $I_{B\max}$ limits may result in restricting the admissible set of solutions for UPFC operating points into a subset of solutions obtained based on applying only the $I_{E\max}$ and $V_{B\max}$ limits.

Other limits can be arbitrarily applied. For example, reactive power supplied by the sending end can be limited; the border of this limit would be represented by a line parallel to $\mathbf{V_S}$. Evaluating effects of the orientation of the series converter is also straightforward. If the series converter is installed in the line segment connected to the sending end, it would suffice to apply the current limit to $\mathbf{I_S}$, instead of to $\mathbf{I_R}$, as was the case here.

The methodology shown in this example can be generalized to solve for all possible operating points of the UPFC. First, the process would be repeated for every $\mathbf{I_E}$ of the given amplitude, that is, for every point of the ellipse. Next, this would be repeated for all $|\mathbf{I_E}| \in [0,\ I_{E\max}]$. Union of all obtained solutions would represent the set of all permissible solutions for the UPFC operating points.

Once all permissible operating points are deduced, those associated with the minimum and maximum power flow are identified. The procedure can be repeated for all values of sending and receiving end voltages (i.e., any angle δ between the two voltages, and P–δ curves for a line controlled by a UPFC can be plotted). Influence of various limits on P–δ curves are demonstrated in the next section.

VII. P–δ Curves

The procedure illustrated in the previous section is used to obtain P–δ curves of a UPFC. The UPFC ratings are selected in an implicit manner to permit a generalized discussion. Following a discussion on the selection of ratings, representative P–δ curves are presented and analyzed. Finally, the moduli of the line currents are plotted as a function of δ. These I_{mod}–δ curves verify that the current limit on the series converter is complied with.

The ratings of the shunt converter are considered first. To select its current rating, the shunt converter is viewed independently as a stand-alone STATCOM (i.e., the series converter is bypassed). The current rating of the STATCOM is uniquely determined by specifying that when installed at the "electrical center" of the line ($k = 0.5$), it is able to maintain 1-p.u. voltage at its terminals when $|\mathbf{V_S}| = |\mathbf{V_R}| = 1$ p.u. and the angle between these vectors is $\delta_{\max}$. This allows the value of $\delta_{\max}$ to be used to specify the STATCOM current ratings. For this analysis, $\delta_{\max}$ is selected at 60°.

The voltage rating of the series converter can be arbitrarily selected. A value of 0.4 p.u. will be used here. The base for the voltage is the nominal line to neutral voltage. Current rating of the series converter is expressed relative to the current that would flow through an uncompensated line at $|\mathbf{V_S}| = |\mathbf{V_R}| = 1$ p.u. at the transmission angle $\delta = 90\ °$.

Such selection of ratings enables easy comparison of P–δ curves for different points of installation (i.e., different values of factor k), different orientations of the series converter, and different values of the series converter current limit.

In this paper, an installation of the UPFC at $k = 0.6$ was considered. In Fig. 11, six P–δ curves are shown, each for a different set of conditions. Curve 1 is the normalized P–δ curve of the uncompensated line. Curve 2 is the P–δ curve of the underlying STATCOM (UPFC when its series converter is bypassed). In contrast to a STATCOM situated in the electrical center of the

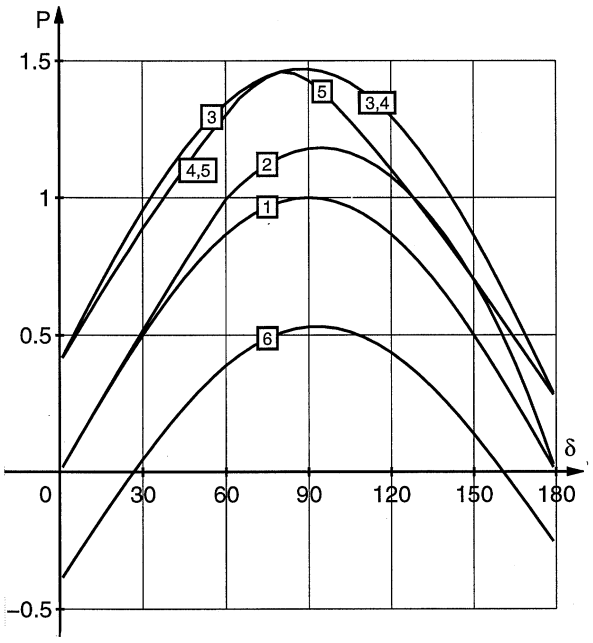

Fig. 11. P–δ curves for the UPFC.

(1) Uncompensated line

(2) $|I_E| \leq 0.379$, $|V_B| = 0$

(3) $|I_E| \leq 0.379$, $|V_B| \leq 0.4$,

(4) $|I_E| \leq 0.379$, $|V_B| \leq 0.4$, $|V_{ET}|$, $|V_{BT}| \leq 1.0$

(5) $|I_E| \leq 0.379$, $|V_B| \leq 0.4$, $|V_{ET}|$, $|V_{BT}| \leq 1.0$, $|I_R| \leq 1.2$

(6) UPFC controlled to minimize the power flow, all limits enforced.

line, curve 2 indicates the transferred power P approaches zero as the angle δ approaches 180°

Curves 3 to 5 are the P–δ curves of the UPFC when controlled to maximize the power flow. For curve 3, the shunt converter current limit and the series converter voltage limit are applied. For curve 4, voltage limits at the UPFC terminals are also added (terminal voltages are limited to 1 p.u.). Curves 3 and 4 clearly demonstrate the capability of the UPFC to increase the power transfer beyond the power transfer achievable by the underlying STATCOM. The difference between curves 3 and 4 exists only at low values of δ, where part of the current capacity of the shunt converter remains unused due to the voltage limits. With no terminal voltage limit (as in curve 3), this capacity is used to increase the power transfer by increasing the voltage at the UPFC terminals.

Curve 5 is the same as curve 4 with the addition of a series converter current limit of 1.2 p.u. The effect of current limiting is visible at higher values of δ. In this region, part of the voltage capacity of the series converter is used to limit the magnitude of current within the $|\mathbf{I_R}| \leq I_{B\max}$ constraint.

Finally, Curve 6 is the P– δ curve of the UPFC when controlled to minimize the power flow through the line. Limit conditions are the same as those used for curve 5.

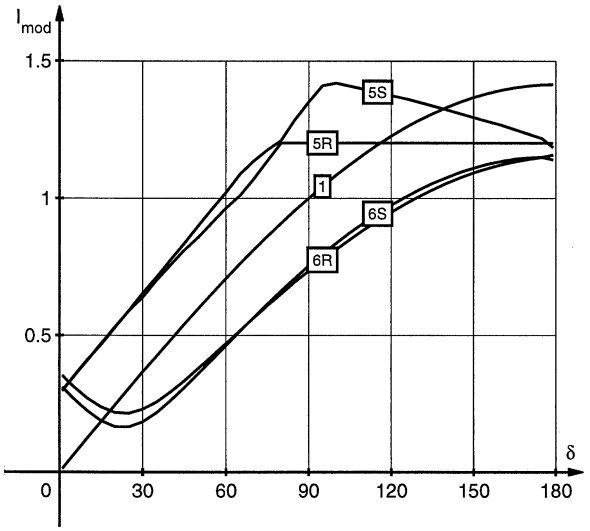

Fig. 12. I_{mod}–δ curves for the UPFC.

(1)	$\lvert I_S\rvert = \lvert I_R\rvert$	Uncompensated line
(5S), (5R)	$\lvert I_S\rvert$, $\lvert I_R\rvert$	$\lvert I_E\rvert \leq 0.379, \lvert V_B\rvert \leq 0.4$, $\lvert V_{ET}\rvert$, $\lvert V_{BT}\rvert \leq 1.0$ $\lvert I_R\rvert \leq 1.2$
(6S), (6R)	$\lvert I_S\rvert$, $\lvert I_R\rvert$	UPFC controlled to minimize the power flow, all limits enforced.

Curves 5 and 6 identify the boundaries of possible operating points for the UPFC. In other words, for any given angle δ between $\mathbf{V_S}$ and $\mathbf{V_R}$, any power transfer between curves 5 and 6 can be realized using the UPFC while imposing limits corresponding to the equipment ratings and terminal voltages. This capability, unique to the UPFC, enables full control of the power transfer through the line and permits decoupled operation of the line from the rest of the system.

A plot of the line current magnitudes, for the conditions of curves 5 and 6 of Fig. 11, is shown in Fig. 12. Suffixes "S" and "R" denote the current through the sending and receiving segments of the line, respectively. Current magnitude of the uncompensated line (curve 1 of Fig. 11) is also shown for comparison.

Fig. 12 demonstrates that the magnitude of the current through the series converter is limited at 1.2 p.u., as specified. Notice that the current magnitude in the sending segment of the line is not limited. This current is free to assume any value.

VIII. Conclusions

A new and systematic method for determining the reachable set of operating points of a UPFC has been presented. The method is general and permits application of all relevant limit conditions: series converter voltage and current limit, shunt converter current limit, and voltage limits at the equipment terminals. The analysis can be performed for any point of installation of the UPFC along a transmission line, and any orientation of the series converter.

The novelties of the proposed method are as follows. First, equal power exchange between shunt and series converters is

achieved by applying a power balance constraint to the transmission line as a whole. This allows the UPFC analysis to be done in the current plane. Second, a manifold of equal power exchange between the converters is defined, and the principle of superposition is used to decompose the circuit. This permits geometric interpretation of the solution composition and gives insight into existence and uniqueness of solutions. Third, a novel coordinate system is introduced which is invariant to the changes of the UPFC operating point, and simplifies the problem of finding extremes of power transfer.

An algorithm for solving the entire possible operating region of a UPFC while applying all relevant limits is also presented. The algorithm is general, and allows for application of limits either individually or collectively. This algorithm is used to solve for the P–δ curves of the UPFC.

The analysis method presented in this paper offers clear insight into how the UPFC equipment ratings affect the line operating limits. Hence, it allows system planners to realistically quantify the benefits of UPFC installation in a given transmission line.

REFERENCES

[1] L. Gyugyi, "Unified power-flow control concept for flexible AC transmission systems," *Proc. Inst. Elect. Eng.—Power Delivery*, pt. C, vol. 139, no. 4, pp. 323–331, July 1992.

[2] ——, "Dynamic compensation of AC transmission lines by solid-state synchronous voltage sources," *IEEE Trans. Power Delivery*, vol. 9, pp. 904–911, Apr. 1994.

[3] R. Mihalic, P. Zunko, and D. Povh, "Improvement of transient stability using unified power flow controller," *IEEE Trans. Power Delivery*, vol. 11, pp. 485–492, Jan. 1996.

[4] A. Nabavi-Niaki and M. R. Iravani, "Steady-state and dynamic models of unified power flow controller (UPFC) for power system studies," *IEEE Trans. Power Syst.*, vol. 11, pp. 1937–1943, Nov. 1996.

[5] J. Bian, D. G. Ramey, R. J. Nelson, and A. Edris, "A study of equipment sizes and constraints for a unified power flow controller," *IEEE Trans. Power Delivery*, vol. 12, pp. 1385–1391, July 1997.

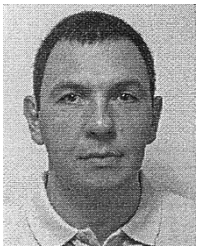

J. Z. Bebic (M'98) received the B.Sc. and M.Sc. degrees in electrical engineering from the University of Belgrade, Yugoslavia, in 1989 and 1994, respectively. He is currently pursuing the Ph.D. degree at the University of Toronto, ON, Canada.

After graduation, he joined the Electrical Engineering Institute "Nikola Tesla" in Belgrade, Yugoslavia, where he held various junior and intermediate engineering positions as a design engineer. From 1994 to 1996, he was a project engineer with North American Rectifier Ltd., Scarborough, ON, Canada. From 1996 to 1999, he was a Power Electronics Engineer with Service Division of Westinghouse Canada, Hamilton, ON, Canada. His current research interest include high power energy converters, converter topologies, and control.

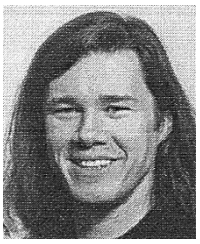

P. W. Lehn (M'99) received the B.Sc. and M.Sc. degrees in electrical engineering from the University of Manitoba, Winnipeg, MB, Canada, in 1990 and 1992, respectively. He received the Ph.D. degree from the University of Toronto, ON, Canada, in 1999.

Currently, he is an Assistant Professor at the University of Toronto. From 1992 until 1994, he was employed by the Network Planning Group of Siemens AG, Erlangen, Germany.

M. R. Iravani (SM'00) received the B.Sc. degree in electrical engineering in 1976 from Tehran Polytechnique University, Iran. He received the M.Sc. and Ph.D. degrees in electrical engineering from the University of Manitoba, Winnipeg, MB, Canada, in 1981 and 1985, respectively.

Currently, he is a Professor at the University of Toronto, ON, Canada. He was a Consulting Engineer from 1976 to 1979. His research interests include power system dynamics and power electronics.